

## Raman Selection Rule Violation for a Spinel Crystal

LEWIS M. FRAAS and JAMES E. MOORE

*Instituto de Física Gleb Wataghin, Universidade Estadual de Campinas', Campinas SP*

Recebido em 5 de Setembro de 1972

Detailed Raman and fluorescence studies were carried out on the crystal system  $\text{MgAl}_2\text{O}_4 : \text{Cr}^{3+}$ . Ten Raman modes, in addition to the five theoretically predicted ones, were observed. The five strongest modes did not obey the Raman selection rules for the host crystal lattice. It is suggested that these anomalies are attributable to impurity resonant Raman effects.

Estudos detalhados dos espectros Raman e fluorescência são feitos em cristal de espinela com impureza de cromo  $\text{MgAl}_2\text{O}_4 : \text{Cr}^{3+}$ . São observados dez picos Raman a mais do que os cinco picos prognosticados teoricamente. Os cinco picos mais fortes não obedecem às regras de Raman de simetria para o cristal de espinela. Sugere-se que estas anomalias sejam atribuídas à ressonância da luz com a impureza.

### 1. Introduction

Raman studies of magnon modes in the spinel crystal,  $\text{CdCr}_2\text{Se}_4$ , have been reported by Harbeke and Steigmeier<sup>1</sup>. However, no detailed Raman polarization studies for the phonon modes of a spinel crystal have been undertaken. It would seem that such studies would be quite useful for future magnon studies. The results of Raman polarization studies for the phonon modes of  $\text{MgAl}_2\text{O}_4$  are reported here and some frequency assignments are made. These results complement phonon mode studies in  $\text{MgAl}_2\text{O}_4$  via host lattice infrared absorption<sup>2</sup>, impurity absorption<sup>3</sup>, and fluorescence<sup>4</sup>, as well as some Raman phonon studies of microcrystalline spinel group minerals<sup>5</sup>.

A normal mode analysis of the vibrations in the spinel structure has been made by Lutz<sup>6</sup>. The polarizability tensors measured for our  $\text{MgAl}_2\text{O}_4$  sample are in violent disagreement with those predicted. These anomalies are attributable to the presence of trace amounts of  $\text{Cr}^{+3}$  impurity. The

---

<sup>†</sup>Postal address: C.P. 1170, 13100 - Campinas SP

detailed analysis of these anomalies is of value quite apart from the spinel structure in view of the current interest in resonant Raman effect.

## 2. Experiment and Results

The crystal studied was obtained through the cooperation of Linde Division, Union Carbide Corpo. It is a synthetic Czochralski grown colorless crystal<sup>17</sup>, considered by the manufacturer to be nearly stoichiometric and nominally pure. The crystal had been cut by the manufacturer along the (111) and (1 $\bar{1}$ 0) axes. This orientation was carefully confirmed by X-ray Laue photographs in our laboratories. The sample was cut and polished in a

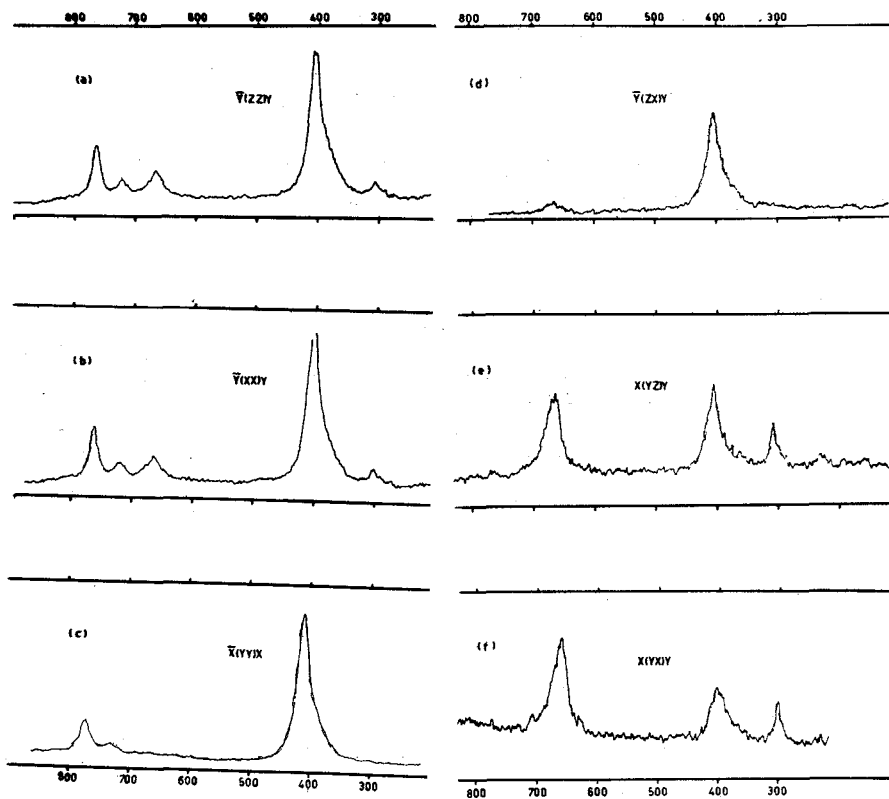


Fig. 1 - Raman polarization spectra of  $MgAl_2O_4$  with Argon laser excitation (a)  $\bar{Y}(ZZ)Y$ , 5145 Å; (b)  $\bar{Y}(XX)Y$ , 5145 Å; (c)  $\bar{X}(YX)X$ , 5145 Å; (d)  $\bar{Y}(ZX)Y$ , 5145 Å; (e)  $X(YZ)Y$ , 5145 Å, high gain; (f)  $X(YX)Y$ , 4880 Å, high gain.

rectangular shape with its face normals as follows:  $x = (111)$ ,  $y = (1\bar{1}0)$  and  $z = (\bar{1}\bar{1}2)$ .

The Raman spectra of Fig. 1 were taken with an Ar ion laser and a Spex double monochromator. The method used is conventional<sup>18</sup>, except that the crystal face normals are not the crystallographic axes. The Raman tensors for the host crystal in the crystallographic axes are transformed to the laboratory axes system, for comparison purposes. The spectra of Fig. 1 were taken with  $8\text{ cm}^{-1}$  spectrometer resolution. In these spectra

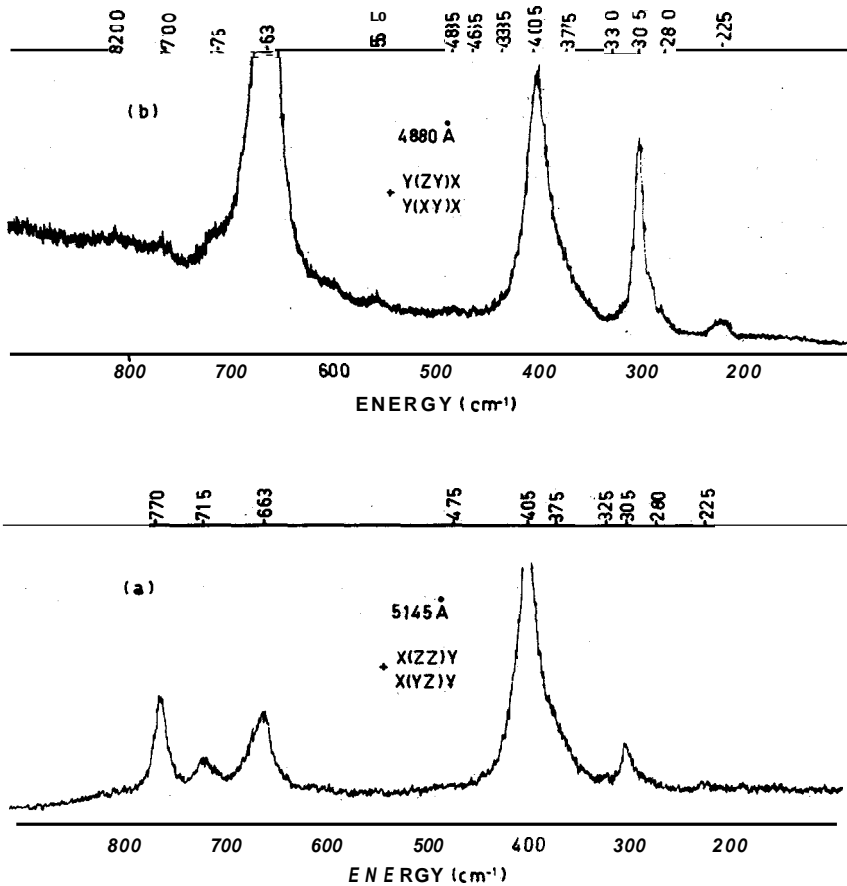


Fig. 2 - High signal Raman spectra of  $\text{MgAl}_2\text{O}_4$ .

there are five reasonably strong lines observed. Group theory predicts for the spinel structure  $1A_{1g}$ ,  $1E_g$ , and  $3F_{2g}$  modes<sup>6</sup>. For the spinel structure, the  $A_{1g}$  modes will always be diagonal regardless of the crystal orientation. This allows identification of  $A_{1g}$  modes immediately. The two modes with the greater frequency shift from the laser line as shown in Fig. 1, can be identified as  $A_{1g}$ . The fact that one observes two  $A_{1g}$  modes instead of one as predicted by group theory led us to look for extra modes. Ten extra modes were found, as can be seen in the high signal to noise spectra shown in Fig. 2. These modes shift with laser frequency when spectra are taken with the 5145 Å and 488 Å Argon laser lines. Thus, all are Raman modes.

In Fig. 2b, the highest signal to noise was observed with the 4880 Å laser line. In these spectra, the Raman lines are seen superimposed on an increasing fluorescence background. This blue-green fluorescence background is a restriction on signal to noise in the 5145 Å spectra of Figs. 1a-e. In addition to the blue-green fluorescence observed with the spectrometer, a bright red fluorescence was easily seen visually in the sample along the laser path. This red light was observed to be most intense with 5145 Å laser excitation.

Spectra of the red and blue-green sample fluorescence were taken at room temperature and liquid nitrogen temperature. These spectra are shown in Fig. 3. The sample was immersed in liquid nitrogen for the 77° K data. The red fluorescence is in agreement with fluorescence from  $Cr^{3+}$  in  $MgAl_2O_4$ , reported elsewhere<sup>4</sup>. All Raman spectra were retaken at liquid nitrogen temperature. These results indicated no appreciable narrowing of the various modes.

A careful comparison of the derived Raman tensors from the data of Fig. 1 shows radical disagreement with theoretical predictions for the other three non  $A_{1g}$  modes. It is noted here that the reliability of these measurements is less since it was necessary to correct the data for the spectrometer polarization preference.

In order to eliminate the possibility of electronic Raman effect from an unknown impurity, as an explanation for some of the observed lines, a slow scan was made through the spectral range from the laser line down to the red fluorescence. No sharp structure was observed. Also, the symmetry of the Raman tensors for the five modes observed was checked. No appreciable asymmetry was found.

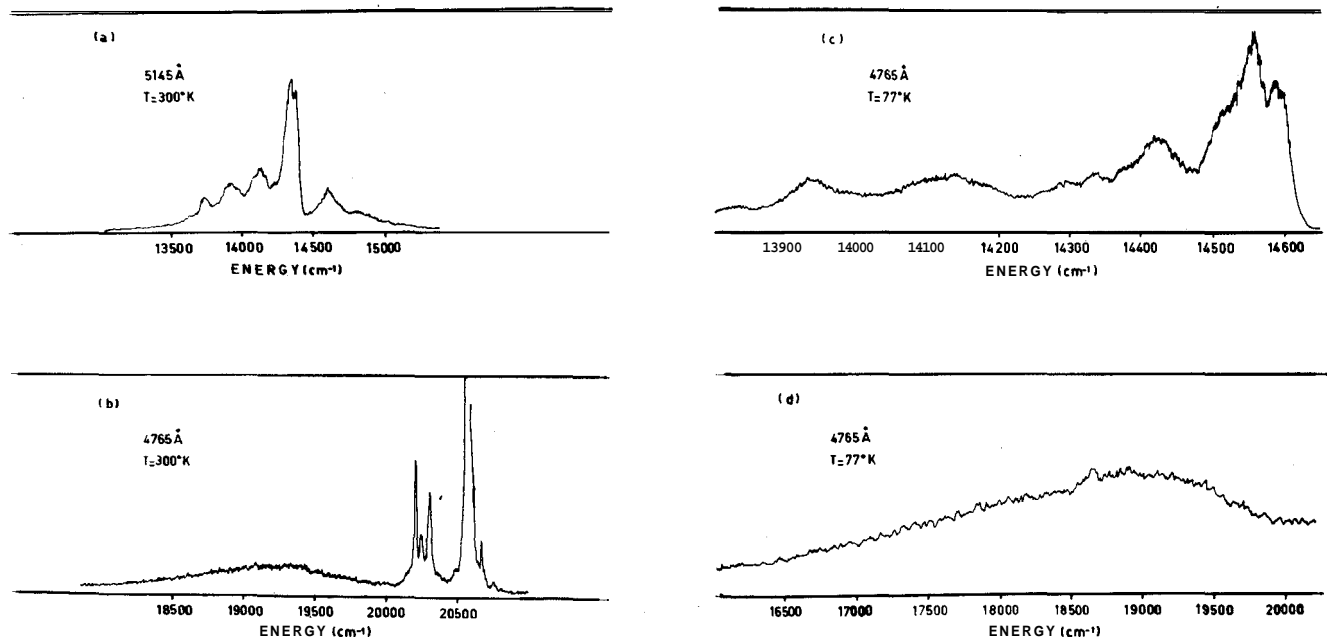


Fig. 3 - Red and green impurity fluorescence spectra of  $MgAl_2O_4 : Cr^{3+}$  at room temperature and liquid nitrogen temperature

In an attempt to explain the anomalies in the polarizability tensors in terms of resonant Raman effect from  $\text{Cr}^{3+}$  impurities, Raman data were taken with the nitrogen laser 3371 Å line as a source. The data are presented in Fig. 4. The lack of availability of polarizers in the ultraviolet region of the spectrum made it impossible to obtain polarization data at 3371 Å. The laser input for Fig. 4a was in the x-direction and Raman light was collected in the y-direction. In Fig. 4b, this geometry was reversed. A resonance effect is observed.

The red fluorescence was also taken with  $N_2$  laser excitation. A secondary fluorescence is observed deeper in the red. The possibility of a rise in this region due to second order visible light was eliminated by use of a red filter. These results are shown in Fig. 4c. This secondary fluorescence is probably due to another impurity<sup>10,11</sup> such as  $\text{Ni}^{2+}$ .

Because of the anomalies in the Raman spectra, sample characterization studies were undertaken. The lattice parameter was measured by means of X-ray analysis and found to be  $8.07 \pm .02$  Å. Linde quotes a lattice parameter of 8.08 Å in good agreement with our value. X-ray fluorescence studies show the following impurities: Ni, Zn, Cu, Fe and Fr.

### 3. Discussion

Before presenting an explanation of the spectra shown in Figs. 1 through 4, it is convenient to discuss in detail the anomalies that were observed.

#### A) Problems with the Raman polarizability tensors:

The spinel unit cell belongs to the cubic space group  $O_h^7(Fd3m)$  with eight formula units per cell. The structure contains two kinds of metal ion sites. The Mg site has tetrahedral coordination with full  $T_d$  symmetry. The Al (or Cr) site has a sixfold distorted octahedral coordination. This site belongs to the  $D_{3d}$  point group. The trigonal axis of the  $D_{3d}$  group is coincident with the (111) axis of the crystal and has a center of inversion. The oxygen sites are  $C_{3v}$ . The irreducible representations for the optical modes of the crystal are:

$$1A_{1g} + 2A_{2u} + 1E_g + 2E_u + 1F_{1g} + 4F_{1u} + 3F_{2g} + 2F_{2u}.$$

Of these, there are five Raman active modes:  $1A_{1g} + 1E_g + 3F_{2g}$ . The Raman tensors in the crystallographic frame of reference are the following:

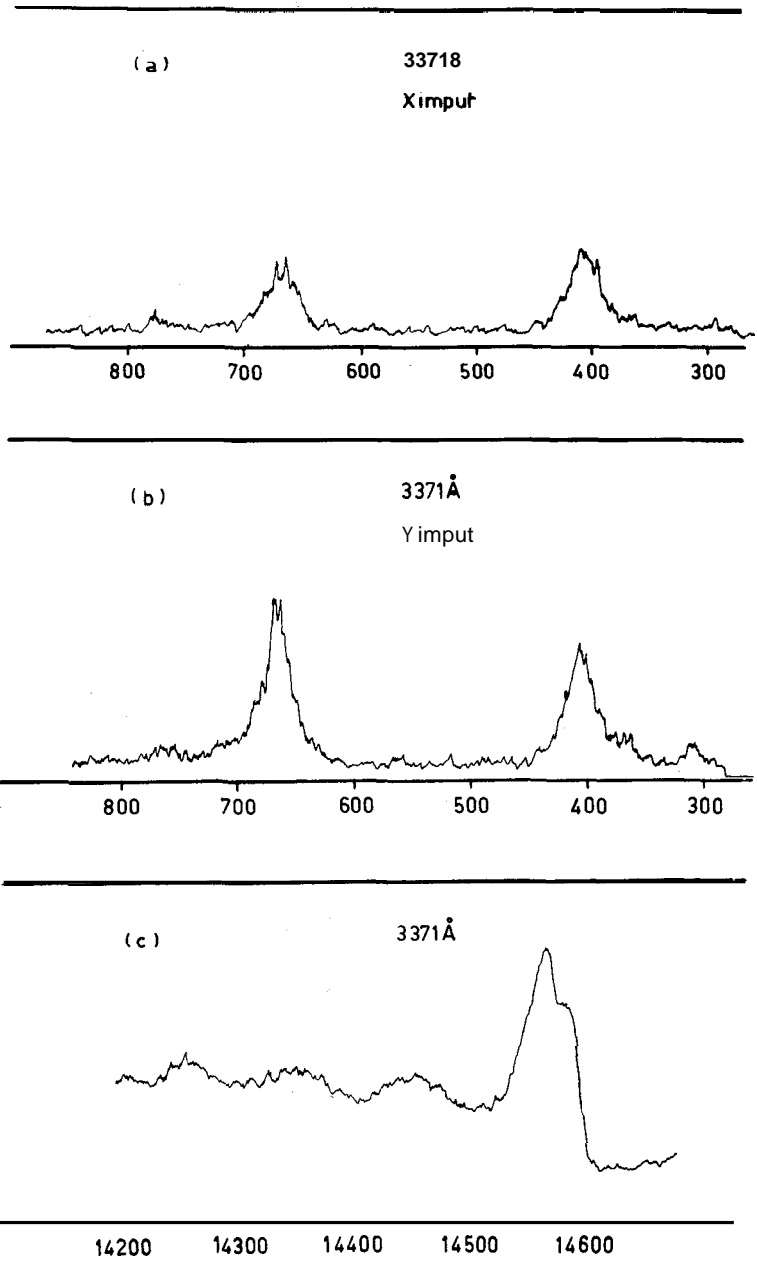


Fig. 4 - Raman and fluorescence spectra of  $MgAl_2O_4$  with nitrogen laser excitation.

$$\begin{aligned}
A_{1g} : a & \begin{bmatrix} 1 & 0 & 0 \\ 0 & 1 & 0 \\ 0 & 0 & 1 \end{bmatrix} \\
E_g : b & \begin{bmatrix} 1 & 0 & 0 \\ 0 & 1 & 0 \\ 0 & 0 & -2 \end{bmatrix}, \quad b\sqrt{3} \begin{bmatrix} 1 & 0 & 0 \\ 0 & -1 & 0 \\ 0 & 0 & 0 \end{bmatrix} \\
F_{2g} : c & \begin{bmatrix} c & 1 & 0 \\ 0 & 0 & 0 \\ 0 & 0 & 0 \end{bmatrix}, \quad c \begin{bmatrix} 0 & 0 & 1 \\ 0 & 0 & 0 \\ 1 & 0 & 0 \end{bmatrix}, \quad c \begin{bmatrix} 0 & 0 & 0 \\ 0 & 0 & 1 \\ 0 & 1 & 0 \end{bmatrix}.
\end{aligned}$$

The transformation tensor to the laboratory frame is:

$$S^{-1} : \begin{bmatrix} 1/\sqrt{3} & 1/\sqrt{2} & 1/\sqrt{6} \\ 1/\sqrt{3} & -1/\sqrt{2} & 1/\sqrt{6} \\ 1/\sqrt{3} & 0 & -2/\sqrt{6} \end{bmatrix}.$$

The transformed polarizability tensors are then given by  $a' = SaS^{-1}$ .

The final  $ij$  intensity components are calculated by summing the squares of the  $ij$  elements of the tensors for the phonons of each symmetry class. For example:

$$a'_{xy}{}^2(E_g) = a'_{xy}{}^2(E_g'') + a'_{xy}{}^2(E_g^b).$$

The results of these calculations are shown in Table I.

MODE	zz	xx	yy	xy	yz	xz
Calculated $F_{2g}$ Intensity	10	13.3	10	3.3	6.7	3.3
Observed #3 Intensity	10	11	<u>0.5</u>	11	19	8
Calculated $E_g$ Intensity	10	0	10	20	10	20
Observed #2 Intensity	10	8.5	15	<u>0.3</u>	<u>0.5</u>	5

Table I - Calculated and Observed Raman Polarization Intensities



If the five modes in Fig. 1 are numbered 1-5 in order of increasing energy shift, then numbers 4 and 5 are seen to have  $A_{1g}$  symmetry. Numbers 1 and 3 behave similarly for Ar laser excitation. Number 2 is **unique**. It would therefore **seem** that modes 1 and 3 are derived from  $F_{2g}$  modes and mode 2 is derived from the  $E_g$  mode. However, there is no confirming evidence for these assignments. The measured polarizabilities for modes 2 and 3 are also shown in Table I. The striking feature in these data is the occurrence of near zeros for  $xy$  and  $yz$  in the number 2 mode and again a near zero in  $yy$  for the number 3 mode. The  $y$ -direction is the  $(1\bar{1}0)$  direction. There is no resemblance for either mode to the tensors for  $E_g$  and  $F_{2g}$ .

### 3.1. Number of Modes

Table II summarizes the mode frequencies found in Fig. 2. Also listed are frequencies observed by other methods. Slack<sup>2</sup> has observed phonon modes in a single crystal of  $MgAl_2O_4$  by means of IR reflectivity. Slack, Ham, and Chrenko<sup>3</sup> have observed lattice phonon modes via optical absorption spectra of tetrahedral  $Fe^{2+}$  in  $MgAl_2O_4$ . Finally, P. P. Kesliuk *et al*<sup>3</sup> have observed lattice phonon modes in the fluorescence spectra of  $Cr^{3+}$

Raman Freq.	Raman Intensity	Crystal IR <sup>a</sup>	$Fe^{2+}$ IR <sup>b</sup>	$Cr^{3+}$ fluof
225 $cm^{-1}$	medium		220	218
280	weak			251
305	*1 strong	302		300
330	weak			
375	shoulder		365	
405	*2 strong			395
435	shoulder		450	447
463	weak	475		
485	weak		500	490
555	weak	530	550	
600	weak	580		
663	*3 strong			650
715	*4 strong			
770	*5 strong	735	775	745
825	weak			

**Table II** - Summary of Spinel ( $MgAl_2O_4$ ) phonon frequency data: a) Ref. 2; b) Ref. 3; c) Ref. 4.

doped  $\text{MgAl}_2\text{O}_4$ . Of the above studies, the Raman spectra of Fig. 2b gives the most complete picture of the phonon spectrum. Fifteen modes are observed.

### 3.2. Nitrogen Laser Resonance

The spectra of Fig. 4 clearly show a resonance. If the intensity ratio of **mode 2** to **mode 3** were the same in the UV as in the visible, then mode 2 should be much stronger in the UV than is observed in Fig. 4. This follows rigorously since the nitrogen laser output is non polarized. In the visible, when the Ar laser frequency is shifted from 5145 Å to 4765 Å, the intensity ratio of **mode 2** to **mode 3** shifts down by 10% (s. Note 12). This shift is in agreement with the nitrogen laser data.

No absorption is observed for pure  $\text{MgAl}_2\text{O}_4$  out to 6ev (Ref. 2). It is therefore concluded that the resonance observed is due to an impurity.

### 3.3 The Pairing Region of the $\text{Cr}^{3+}$ Fluorescence Spectrum

The room temperature and liquid nitrogen temperature fluorescence spectra of Fig. 3 are in substantial agreement with the spectra reported by Wood *et al*<sup>4</sup>. The sharp rise occurs at  $14\,600\text{ cm}^{-1}$  at  $77^\circ\text{ K}$  for both cases. Vibronic structure is observed at  $745\text{ cm}^{-1}$ ,  $650\text{ cm}^{-1}$ ,  $490\text{ cm}^{-1}$ ,  $447\text{ cm}^{-1}$ ,  $395\text{ cm}^{-1}$ , etc. in both cases, on the low frequency side of  $14\,600\text{ cm}^{-1}$  at  $770^\circ\text{ K}$ . Furthermore, identical structure is observed on the high frequency side of  $14\,600\text{ cm}^{-1}$  at room temperature in both cases. The one area of disagreement is in the region on the low frequency side of  $14\,600\text{ cm}^{-1}$  for small energy shifts between 0 and  $200\text{ cm}^{-1}$ . This is the region where Wood *et al.* reported N lines associated with  $\text{Cr}^{3+}$  pairs. Our spectra show anomalous structure in this region. This structure is of high intensity, in fact higher intensity than the  $\text{Cr}^{3+}$  R line intensity. These features are somewhat broad and do not correspond in detail to the N lines from  $\text{Cr}^{3+}$  pairs.

## 4. Interpretation

*A priori*, there are three possible explanations for the anomalies described in the previous section. The first is  $\text{Cr}^{3+}$  resonance. The second is nonstoi-

chiometry. And the third is complete disorder in the **Mg-Al** positions. We feel that the nonstoichiometry cannot be large enough to account for the near zeros observed in the data of Table I. A 50% nonstoichiometry would yield a 50% disagreement between intensity measurement and **pre**dictions and not the observed zeros. There is no **evidence** for complete disordering in the literature for synthetic **MgAl<sub>2</sub>O**. Neither nonstoichiometry or complete disordering can account for the resonance observed. Therefore the anomalies are probably attributable to the **Cr<sup>3+</sup>** resonance.

The observed Raman tensors for the modes numbered 2 and 3 have the following forms:

$$*2 : \begin{bmatrix} - & 0 & - \\ 0 & - & 0 \\ - & 0 & - \end{bmatrix}, \quad *3 : \begin{bmatrix} - & - & - \\ - & 0 & - \\ - & - & - \end{bmatrix}.$$

The remaining problem is to explain the obvious importance of the  $(\bar{1}\bar{1}0)$  axes. If **Cr<sup>3+</sup>** were simply substituted in the place of **Al<sup>3+</sup>**, the impurity site created would have  $D_{3d}$  symmetry and thus a C<sub>3</sub> axis. Since this C<sub>3</sub> axis lies along the (111) direction, the zeros along the  $(\bar{1}\bar{1}0)$  direction are not explained. If however, a **Cr<sup>3+</sup>** were to preferentially substitute for **Al<sup>3+</sup>** ions near **Mg<sup>2+</sup>** vacancies, the **Mg<sup>2+</sup>** vacancy pair would have its highest symmetry element, a **reflection** plane, along the  $(\bar{1}\bar{1}0)$  axis. Such a pair could explain as well the anomaly in the pairing region of our sample's fluorescence.

## 5. Conclusions

Because of the large number of ferrite spinels, the utility of the phonon frequency information obtained here is **apparent**. This paper also shows that polarization studies can give information about the resonant Raman effect from impurity sites even in the case of broad absorption bands. Specifically, this applies to the case when the impurity site symmetry is lower than the host lattice symmetry. This paper also shows that the **reverse** of this statement is true, that is, Raman polarization studies of impurity **mode** spectra in the resonant region **can** give information about impurity site symmetry.

The authors are grateful for the technical **assistance** in crystal preparation of Marcelo Fossey. The help of Dr. José Salzberg with the X-ray Laue and **fluorescence** work is also **gratefully** acknowledged. We also appreciate the cooperation of Prof. Nicolao **Jannuzzi** in connection with the **N<sub>2</sub>** laser work reported here.

## References and Notes

1. E. F. Steigmeier, G. Harbeke, Phys. Cond. Matter **12**, 1 (1970).
2. G. A. Slack, Phys. Rev. **134**, A1268 (1964).
3. G. A. Slack, F. A. Ham, R. M. Chrenko, Phys. Rev. **152**, 376 (1966).
4. D. L. Wood, G. F. Imbush, R. M. Macfarlane, P. Kesliuk, D. M. Larkin, J. Chem. Phys. **48**, 5255 (1968).
5. W. P. Griffith, J. Chem. Soc. (A), 286 (1970).
6. H. D. Lutz, Z. Naturforsch. **24a**, 1417 (1969).
7. Crystal Products Bulletin, Union Carbide Corp., Czochralski Spinel
8. T. C. Damen, S. P. S. Porto, B. Tell., Phys. Rev. **142**, 570 (1966).
9. However, the axes chosen are most convenient for impurity site symmetry analysis.
10. J. E. Ralph, M. G. Townsend, Mullrsd. Research Labs. Report \*M306.
11. J. E. Ralph, M. G. Townsend, J. Chem. Phys. **48**, 149 (1968).
12. The spectrometer polarization preference changed as well but this correction was made.